G-CSF/SCF reduces inducible arrhythmias in the infarcted heart potentially via increased connexin43 expression and arteriogenesis

Michael T. Kuhlmann,[1] Paulus Kirchhof,[1,2] Rainer Klocke,[1] Lekbira Hasib,[1] Jörg Stypmann,[1,2] Larissa Fabritz,[1,2] Matthias Stelljes,[3] Wen Tian,[1] Melanie Zwiener,[1,2] Marcus Mueller,[4] Joachim Kienast,[3] Günter Breithardt,[1,5] and Sigrid Nikol[1]

[1]Department of Cardiology and Angiology, [2]Interdisciplinary Center for Clinical Research Münster, [3]Department of Medicine/Hematology and Oncology, [4]Department of Neurology, and [5]Leibniz Institute for Arteriosclerosis Research, University of Münster, 48129 Münster, Germany

Granulocyte colony-stimulating factor (G-CSF), alone or in combination with stem cell factor (SCF), can improve hemodynamic cardiac function after myocardial infarction. Apart from impairing the pump function, myocardial infarction causes an enhanced vulnerability to ventricular arrhythmias. Therefore, we investigated the electrophysiological effects of G-CSF/SCF and the underlying cellular events in a murine infarction model.

G-CSF/SCF improved cardiac output after myocardial infarction. Although G-CSF/SCF led to a twofold increased, potentially proarrhythmic homing of bone marrow (BM)-derived cells to the area of infarction, <1% of these cells adopted a cardial phenotype. Inducibility of ventricular tachycardias during programmed stimulation was reduced 5 wk after G-CSF/SCF treatment. G-CSF/SCF increased cardiomyocyte diameter, arteriogenesis, and expression of connexin43 in the border zone of the infarction. An enhanced expression of the G-CSF receptor demonstrated in cardiomyocytes and other cell types of the infarcted myocardium indicates a sensitization of the heart to direct influences of this cytokine. In addition to paracrine effects potentially caused by the increased homing of BM-derived cells, these might contribute to the therapeutic effects of G-CSF.

CORRESPONDENCE
Sigrid Nikol:
nikol@uni-muenster.de

Abbreviations used: BMT, BM transplantation; ECG, electrocardiogram; EGFP, enhanced green fluorescent protein; G-CSF, granulocyte colony-stimulating factor; LAD, left anterior descending coronary artery; MAP, monophasic action potential; SCF, stem cell factor

Myocardial infarction is responsible for about one third of heart failure cases (1–3). It is defined as the loss of myocardial tissue that is replaced by scar tissue (4, 5). The formation of scar tissue is not only one of the most important factors compromising the pump function of the failing heart, but it is also an important risk factor for ventricular arrhythmias because it constitutes anatomical conduction barriers that cause electrical reentrant circuits. Ventricular tachyarrhythmias are the main cause for sudden death in heart failure patients (4–6). Therefore, new approaches for the therapy of heart failure should not only improve hemodynamic function, but they should also aim at a reduction of the vulnerability to arrhythmias.

Initial preclinical and clinical trials have demonstrated that the transfer of BM-derived stem and precursor cells into the infarcted myocardium can improve left ventricular systolic function (7–9). Similar results were obtained by the application of the cytokine granulocyte colony-stimulating factor (G-CSF), alone or in combination with stem cell factor (SCF), which is known to mobilize BM-derived cells (10–14). The publications of Orlic et al. (10, 15, 16) suggest that the beneficial effects of these therapies are due to a significant degree of structural regeneration of the infarcted hearts by transdifferentiation of the immigrated BM-derived cells to cardiomyocytes. In contrast, others (17–19) were unable to reproduce these results. However, recent data by Gnecchi et al. (20) indicate that paracrine (humoral) factors secreted by BM-derived cells promote cardiomyocyte survival. Recently, a

M.T. Kuhlmann and P. Kirchhof contributed equally to this work.

The online version of this article contains supplemental material.

new aspect was added by the work of Harada et al. (14), who identified direct effects of G-CSF on cardiomyocytes in vitro.

However, the mere increase of BM-derived cells in the infarcted heart by cytokine treatment as well as their potential transdifferentiation into noncardiomyocytes or even cardiomyocytes might carry a risk for pro-arrhythmia. The transfer of skeletal myoblasts into failing hearts has been shown to provoke ventricular tachycardias in patients (21), and certain types of cardiomyocytes derived from in vitro–differentiated embryonic stem cells exhibited prolonged action potential durations, afterdepolarizations, and a potential for arrhythmogenesis (22). On the other hand, reducing the infarct size has the potential to reduce the risk of ventricular arrhythmias after myocardial infarction. Therefore, the aim of this study was to systematically evaluate the midterm electrophysiological effects of G-CSF/SCF treatment on hearts subjected to myocardial infarction, and to reveal cellular changes potentially underlying the observed physiological alterations.

RESULTS

G-CSF/SCF promotes the homing of enhanced green fluorescent protein (EGFP)$^+$ cells in the infarcted left ventricle of mice

The homing of BM-derived cells to the infarcted myocardium on the one hand might contribute to the beneficial effects of G-CSF/SCF by paracrine mechanisms. On the other hand, it might constitute the cellular basis for an enhanced susceptibility to arrhythmia. Because of these notions, the homing of BM-derived cells was comparatively analyzed in G-CSF/SCF-treated and untreated infarcted hearts.

EGFP-transgenic donor mice were used for BM transplantation (BMT) into irradiated recipient animals before these were subjected to infarction and G-CSF/SCF treatment. As expected, ligation of the left anterior descending coronary artery (LAD) caused anterior myocardial infarction as evident by replacement of myocardium with fibrotic scar tissue 5 wk after the infarction (Fig. 1 A). Morphometric analysis of the hearts of 15 BMT animals (4 G-CSF/SCF treated and 11 untreated) killed 5 wk after induction of myocardial infarction identified EGFP$^+$ (BM-derived) cells predominantly in the area of myocardial infarction and its border zone (Fig. 1 B). Furthermore, G-CSF/SCF led to a twofold increase of homing of EGFP$^+$ cells to the infarcted area and the border zone of myocardial infarction ($P < 0.05$ for G-CSF/SCF vs. controls). In agreement with this finding, G-CSF/SCF led to a threefold rise in white blood cell concentration in the peripheral blood, accompanied by a doubling of the neutrophil proportion in splenectomized mice (not depicted). In 10 BMT animals not subjected to infarction (five G-CSF/SCF treated and five untreated), the accumulation of EGFP$^+$ cells 5 wk after G-CSF/SCF treatment was 4–6-fold lower than in the non-infarcted myocardial tissue of animals with myocardial infarction (Fig. 1 B).

98–99% of EGFP$^+$ cells in the myocardium were white blood cells as evident by coimmunolocalization of CD45

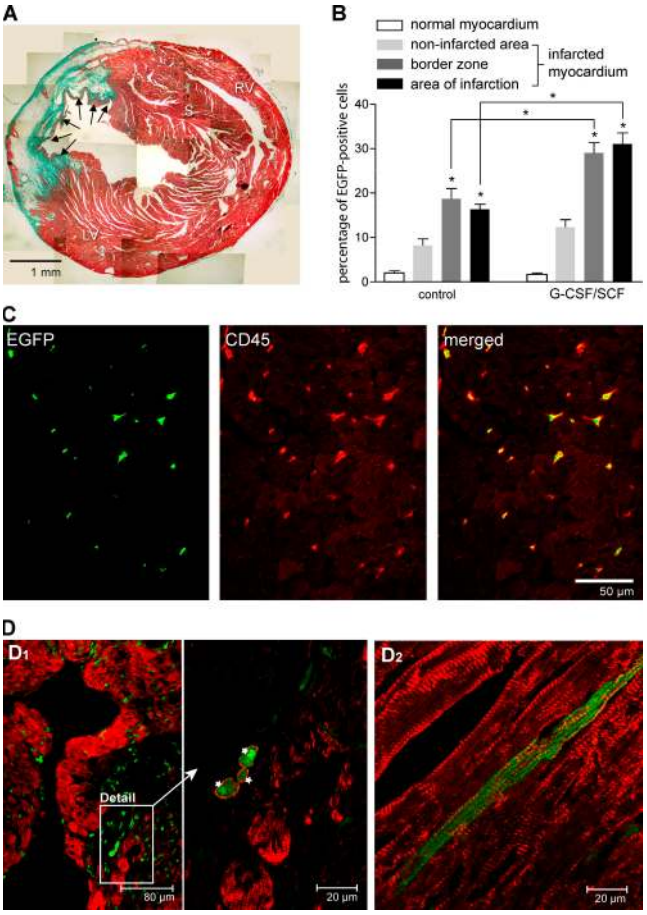

Figure 1. Homing of BM-derived cells in the infarcted myocardium. (A) Histological reconstruction of a short axis cut of the left ventricle after myocardial infarction seen in Goldner's Trichrom stain. The infarcted area (top left quadrant of the section, arrows) is characterized by thinning of the left ventricular wall and replacement of myocardium with fibrotic tissue (green) and inflammatory cells. A subendocardial layer of myocardium survived after myocardial infarction. LV, left ventricle; RV, right ventricle; S, septum. (B) Quantitative analysis of EGFP$^+$ cells in the infarcted and non-infarcted regions as well as in the border zone of G-CSF/SCF-treated and untreated hearts 5 wk after induction of myocardial infarction. Also, percentages of EGFP$^+$ cells in the hearts of G-CSF/SCF-treated and untreated EGFP BM chimeras not subjected to infarction are indicated. Asterisks above bars indicate statistically significant differences of percentages of EGFP$^+$ cells between the border zone or area of infarction and non-infarcted areas of the same animals for controls or G-CSF/SCF mice ($P < 0.05$). Asterisks above parentheses indicate significant differences between the border zone or area of infarction of controls and G-CSF/SCF group. (C) Colocalization (right) of EGFP fluorescence (left) and CD45 immunofluorescence (middle) indicates that the majority of BM-derived cells are white blood cells. (D) Green fluorescent cardiomyocytes (*) in the scar tissue of a G-CSF/SCF animal (D1) and the non-infarcted area of a non–G-CSF/SCF animal (D2) 5 wk after induction of myocardial infarction in recipients of EGFP-expressing BM. Intact cardiomyocytes are labeled by immunofluorescence for troponin T using a red fluorochrome (Alexa Fluor 594). The green color represents the autofluorescence of EGFP$^+$ (BM-derived) cells.

(Fig. 1 C), regardless of location (infarcted vs. non-infarcted area), and protocol type (G-CSF/SCF vs. control). In >100 sections from the hearts of G-CSF/SCF and control animals, only one troponin T^+/$EGFP^+$ cell with central nucleus, myofilaments, and cross-striation (Fig. 1 D) was identified in an area of infarction. In the non-infarcted areas, troponin T^+/$EGFP^+$ cells were casually found (up to five cells per cross section).

G-CSF receptor (G-CSFR) is expressed in several cell types of the heart and is up-regulated by infarction

Because G-CSF and SCF were administered systemically, expression of the corresponding receptors was analyzed in the heart to find evidence for potential direct effects on myocardial tissue. G-CSFR expression was evaluated by immunofluorescence microscopy 1 d and 5 wk after induction of myocardial infarction as well as by quantitative real-time RT-PCR at six time points after infarction. 1 d after myocardial infarction, prominent G-CSFR expression in the non-infarcted area was predominantly detected in small interstitial and vascular cells (Fig. 2 A, 1), whereas in the infarcted area, cardiomyocytes also exhibited weak G-CSFR immunofluorescence (Fig. 2 A, 2). In contrast, 5 wk after induction of myocardial infarction, cardiomyocytes exhibited marked G-CSFR expression both in the non-infarcted area and in the border zone (Fig. 2 A, 3 and 4). Cardiomyocytes, immunopositive for G-CSFR, display a bright red corona, indicating membrane localization of the receptor. Animals investigated 1 d after myocardial infarction were chimeras with EGFP-expressing BM (see Materials and methods). Because the small interstitial cells, immunopositive for G-CSFR, were not $EGFP^+$, these cells were not of hematopoietic origin but were resident myocardial cells. In contrast to G-CSFR, the receptor for SCF (c-kit) was not

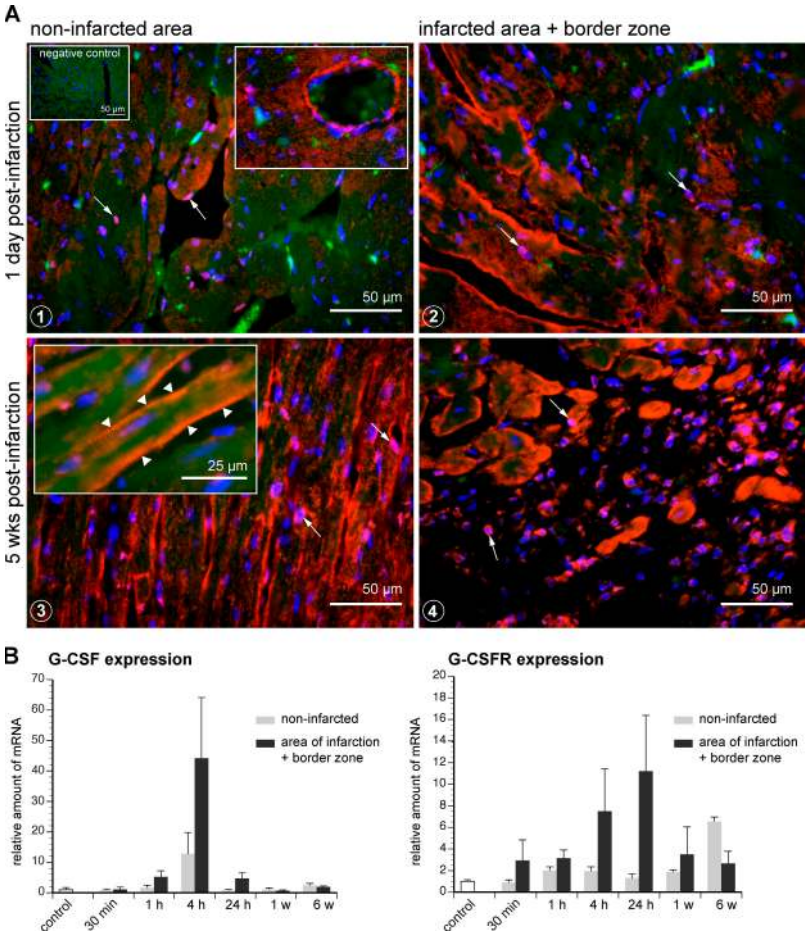

Figure 2. G-CSF/GCSFR expression in the myocardium. (A) G-CSFR expression 1 d (1 and 2) and 5 wk (3 and 4) after induction of myocardial infarction. Blue, DAPI-stained nuclei; bright green, EGFP emission; dark green, autofluorescence of cardiomyocytes; red, Cy3-labeled G-CSFR. Arrows indicate small interstitial cells. Right box in panel 1 indicates a $G\text{-}CSFR^+$ vessel. Arrowheads in panel 3: Bright red corona, indicating membrane localization of the receptor. Immunopositive interstitial cells appear pink (arrows) because of their high nucleus/plasma ratio and the interference of blue DAPI emission (nucleus) and the red Cy3 emission of the G-CSFR label. (B) Expression of G-CSF mRNA and G-CSFR mRNA as determined by real-time RT-PCR at different time points after induction of myocardial infarction in the area of infarction and non-infarcted left ventricular tissue of untreated animals. Left ventricular tissue of seven normal animals (no myocardial infarction and no G-CSF/SCF) served as control.

detectable by immunofluorescence 5 wk after myocardial infarction (not depicted).

Real-time RT-PCR analysis of myocardial tissue of untreated animals revealed an up-regulation of G-CSF and G-CSFR mRNA levels within the first 24 h after induction of myocardial infarction, which was more pronounced in the affected tissue than in the non-infarcted area (Fig. 2 B).

G-CSF/SCF improves hemodynamic function

Myocardial infarction induced by LAD ligation led to regional wall motion abnormalities of the anterior wall, reduced fractional shortening, and typical electrocardiogram (ECG) changes seen after anterior myocardial infarction in the mouse (Fig. 3, A and B). Infarction size was relatively homogeneous throughout the experiments and did not differ between G-CSF/SCF hearts and controls, neither in pathological measurements (Table I) nor in vivo, assessed by the akinetic area of the left ventricle on echocardiography (G-CSF/SCF treated 5.4 ± 0.8 mm^2 vs. controls 6.7 ± 1.1 mm^2; P = 0.39). Also, left ventricular contractility did not differ between G-CSF/SCF-treated mice and controls. It is worthy to note that fractional shortening showed a trend toward better function, and septal wall width bordering the area of myocardial infarction showed a trend toward greater thickness in G-CSF/SCF mice. Despite the lack in infarct size reduction, cardiac output was significantly increased in G-CSF/SCF mice compared with controls (Fig. 3 C).

G-CSF/SCF does not provoke afterdepolarizations and spontaneous ventricular tachycardias in the intact heart

Based on reports of proarrhythmic effects provoked by the transplantation of skeletal myoblasts (21), the proarrhythmic risk of the increased homing of BM-derived cells was assessed by observing spontaneous ventricular rhythm after atrioventricular nodal block (23–25). This protocol did not provoke more spontaneous arrhythmias in G-CSF/SCF-treated hearts compared with controls (7 out of 25 G-CSF/SCF-treated hearts with spontaneous arrhythmias vs. 7 out of 26 controls; P = NS). Furthermore, ventricular action potential durations were shorter in G-CSF/SCF mouse hearts when pacing rates were high, whereas action potential

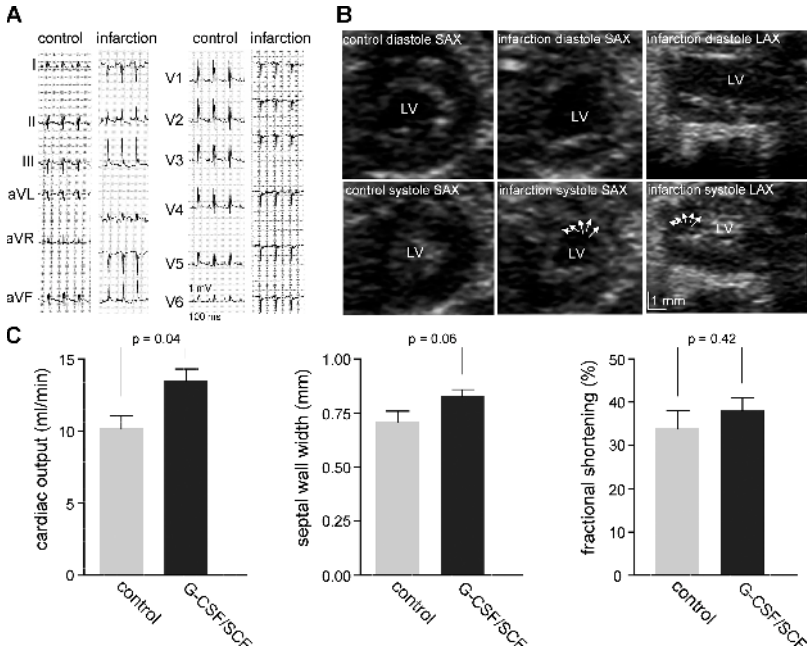

Figure 3. Surface ECG and echocardiographic examination of left ventricular function 5 wk after experimental infarction (A and B) and hemodynamic characterization of G-CSF/SCF–treated hearts compared with controls (C). (A) 12-lead surface ECGs recorded before (left panels, control) and 3 wk after infarction (right panels, infarction). The typical signs of infarction, loss of R waves in the Einthoven leads and persistent ST segment elevation suggestive of anterior left ventricular dyskinesia, are present. (B) Echocardiographic examination before and 3 wk after experimental myocardial infarction in short axis (SAX, middle panels, orientation similar to the histological cut depicted in B) and long axis views (LAX, right panels) recorded during diastole (top panels) and systole (bottom panels). Arrows indicate the hypokinetic area in the systolic pictures. (C) Comparative analysis of hemodynamic functions of G-CSF/SCF-treated and untreated hearts. A statistically significant difference was observed for cardiac output (left). Septal wall width bordering the area of myocardial infarction displayed a trend toward greater thickness (middle), and fractional shortening (basal left ventricular M mode) showed a trend toward better function (right). For the following parameters no differences between G-CSF/SCF and control could be assessed: heart rate during echocardiography: aortic Doppler velocity and left ventricular ejection time; basal left ventricular M mode: posterior wall width, left ventricular enddiastolic diameter and left ventricular endsystolic diameter; mid-left ventricular M mode: septal wall width, left ventricular enddiastolic diameter, left ventricular endsystolic diameter, and fractional shortening.

Table I. General physical and gross pathological parameters in mice treated with G-CSF/SCF or placebo (controls)

	G-CSF/SCF	Controls	P-value
Age (weeks)	24 ± 1.8	26 ± 2.1	0.49
Weight (g)	35.6 ± 1.4	35.3 ± 1.6	0.9
Heart rate during echocardiography (b/min)	434 ± 26	378 ± 26	0.14
Stroke Volume (μl)	32.5 ± 2.1	28.7 ± 1.7	0.17
Infarct length (mm; $n = 10$ per group)	5.4 ± 0.4	5.4 ± 0.2	0.82
Infarct width (mm; $n = 9$ per group)	4.8 ± 0.3	4.7 ± 0.4	0.71
Infarct area (length × width)	26.8 ± 3.2	25.0 ± 2.2	0.65
Left atrial diameter (mm)	2.3 ± 0.2	2.2 ± 0.2	0.58
LVOT diameter	1.1 ± 0.02	1.1 ± 0.02	0.65

All values are given as mean ± SEM. Functional parameters are assessed by echocardiography.

durations were not different between groups during long pacing cycle lengths (Table II).

G-CSF/SCF reduces inducibility of ventricular arrhythmias and increases connexin43 expression

Ventricular arrhythmias after myocardial infarction are often a result of conduction slowing in the border zone of the infarcted myocardium and associated with decreased intercellular connections in this region (26). Programmed stimulation, the best assay to provoke such reentrant arrhythmias, provoked less ventricular tachycardias in G-CSF/SCF-treated mice when either a single premature extra stimulus (Fig. 4 A, top) or two consecutive premature stimuli (Fig. 4 A, bottom) were applied (Fig. 4 B). As expected, a reduction of connexin43 expression (90% reduction) was found in the border zone of the infarction (Fig. 4 C and Videos S1–S4, available at http://www.jem.org/cgi/content/full/jem.20051151/DC1), consistent with conduction slowing, the hallmark of inducible ventricular arrhythmias after myocardial infarction. G-CSF/SCF-treated hearts, in contrast, had markedly higher connexin43 levels in the border zone of the infarction when compared with untreated controls (25% of normal connexin43 levels; Fig. 4 C and Videos S1–S4).

Table II. Electrophysiology—ventricular action potential durations at 90% repolarization (APD90) for different pacing rate lengths in mice treated with G-CSF/SCF or placebo (controls)

APD90	G-CSF/SCF	Controls
at 100 ms	31.1 ± 1.2 ms	35.6 ± 0.7 ms[a]
at 120 ms	33.9 ± 1.5 ms	35.8 ± 1.0 ms
at 140 ms	38.8 ± 1.4 ms	36.2 ± 1.1 ms

All values are given as mean ± SEM. Ventricular action potential durations at 50 and 70% repolarization showed no differences between treatment groups (unpublished data).
[a]A significant difference ($P < 0.05$).

G-CSF/SCF increases arteriogenesis and cardiomyocyte hypertrophy in the border zone of infarction

G-CSF/SCF enhanced arterialization in the border zone of myocardial infarction as indicated by an increased number of vessels per field of view (Fig. 5 A). However, concordant with increased arteriogenesis, the mean vessel diameter was not affected. Cardiomyocyte hypertrophy was more pronounced in the border zone of the infarction after G-CSF/SCF treatment (Fig. 5 B).

DISCUSSION

Main findings

G-CSF/SCF treatment increased the homing of BM-derived cells (mainly white blood cells) into the infarcted myocardium twofold. In addition, up-regulation of G-CSFR expression in the infarcted myocardium suggests a sensitization for direct effects of the cytokine. G-CSF/SCF increased cardiac output regardless of infarction size and integration of BM-derived cells into the myocardium. G-CSF/SCF reduced the inducibility of ventricular arrhythmias. This antiarrhythmic effect can be attributed to an increased expression of connexin43 in cardiomyocytes in the border zone of the infarction. Although provocation of afterdepolarizations was a specific aim of this study, there was no tendency for spontaneous arrhythmias or afterdepolarizations after G-CSF/SCF treatment. The observed physiological effects of cytokine treatment were associated with cardiomyocyte hypertrophy and an enhanced arterialization in the border zone of the infarction.

Primary mechanisms of G-CSF/SCF effects

G-CSF/SCF treatment resulted in an increased homing of BM-derived cells (mainly white blood cells) into the infarcted myocardium and its border zone. In agreement with Murry et al. (17), Balsam et al. (18), and Nygren et al. (19), because a significant degree of transdifferentiation was not observed, this allows us to speculate that the observed therapeutic effects may be due to the secretion of stimulatory factors by white blood cells. However, the debate as to how G-CSF/SCF-based cardiac regenerative therapies improve cardiac function (10, 15–16), and whether transdifferentiation of BM-derived cells is the underlying mechanism of myocardial regeneration (27, 28), has recently been extended by Harada et al. (14). Their results indicate a significant survival-promoting effect of G-CSF treatment on cardiomyocytes and endothelial cells that prevented left ventricular remodeling after myocardial infarction, suggesting that G-CSF may directly act on cardiomyocytes and endothelial cells. However, in contrast to Orlic et al. (10) and our work, they did not use splenectomized mice for their experiments. Differences in neutrophil accumulation in the blood between splenectomized and nonsplenectomized mice might explain why they were unable to identify differences between the homing of BM-derived cells in G-CSF–treated and control hearts. Although the threefold rise in white blood cell count in peripheral blood measured in our G-CSF/SCF–treated

animals is in the range observed in nonsplenectomized animals (29), the boost in the proportion of neutrophils is less pronounced in nonsplenectomized animals (not depicted). Nevertheless, Adachi et al. (30), who also did not use splenectomized animals for their experiments, reported an increased infiltration of BM-derived side population cells into the G-SCF–treated infarcted heart. Together with recent data (20) about the secretion by BM-derived mesenchymal stem cells of so far unknown paracrine factor(s), capable of reducing the infarct size in a rat model of permanent coronary artery occlusion, their results demonstrate that the question of the relative contribution of direct and paracrine effects to the therapeutic action of G-CSF is not definitely answered.

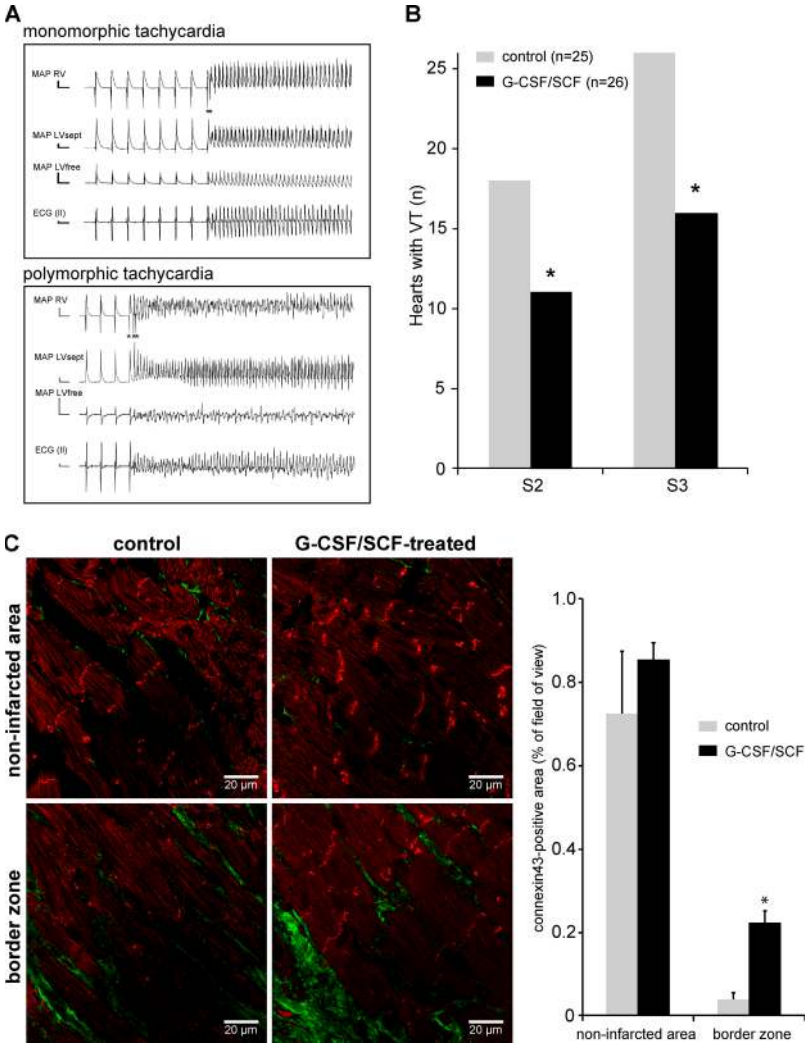

Figure 4. (A) Examples of monomorphic (top) and polymorphic (bottom) ventricular tachycardia induced by programmed stimulation using a single (top) or two (bottom) extra stimuli. Shown are three simultaneously recorded MAP recordings obtained from the right ventricular (MAP RV), left ventricular septal (MAP LVsept), and left ventricular free wall (MAP LVfree) epicardium. In the lower panel, the left ventricular free wall is recorded from the infarcted area and shows the typical alterations found in infarcted scar tissue: loss of the action potential dome and slow activation. Asterisks indicate stimulus artifacts in the right ventricular MAP recording. (B) Number of hearts with induced ventricular tachycardias (>10 consecutive premature ventricular activations) as a function of the number of extra stimuli (S2, first extra stimulus; S3, second extra stimulus) shown for hearts with G-CSF/SCF (black bars) and hearts from non-G-CSF/SCF control animals (gray bars). Ventricular tachycardia induction was less likely in G-CSF/SCF-treated hearts than in controls. (C) Left: Representative immunohistological sections of normal myocardium (top panels) and the border zone of the infarction (bottom panels) in untreated (left panels) and G-CSF/SCF-treated (right panels) hearts. Bright red immunofluorescence, connexin43; dark red, autofluorescence of myocytes; green, immunofluorescence detection of a fibrous tissue marker (rat anti-reticular fibroblast antibody; refer to Materials and methods, and see supplemental Materials and methods for a 3D visualization of connexin43 localization in the intercellular connections). Right (diagram): Mean connexin43 expression measured as connexin43^{+} area in relation to the whole area of myocardial tissue in the field of view. Connexin43 expression was markedly reduced in the border zone of the myocardial infarction. G-CSF/SCF increased connexin43 expression in the border zone without affecting connexin43 expression in normal myocardium.

Our results regarding G-CSFR expression are in agreement with Harada et al. (14) as well as Schneider et al. (31) and suggest that the infarcted myocardium is sensitized for direct effects of G-CSF by an increased expression of the G-CSFR. Together with the parallel increase of local G-CSF expression after myocardial infarction (Fig. 2 B), these data suggest the existence of an endogenous mechanism of G-CSF signaling activation potentially mediating cardioprotective effects. Similar results were obtained in a model of brain infarction (31). However, in view of the twofold-increased homing of BM-derived cells, they also do not allow to favor one of the explanations (paracrine vs. direct effects) but leave the alternative open that both mechanisms act in parallel. Nevertheless, the recent observation of a rise of G-CSF concentration in the blood accompanied by an increase of peripheral $CD34^+$ cells (endothelial progenitor cells) after acute myocardial infarction in humans (32) allows us to speculate that myocardial damage by itself leads to the activation of an endogenous BM mobilization mechanism, possibly enhancing the recruitment of BM-derived cells from the blood.

Improvement of cardiac output

Concordant with results from some (33), but not all (14), groups, we found no change in infarct size after G-CSF/SCF treatment. In addition, we did not find evidence for the generation of new myocardium after G-CSF/SCF treatment. Cardiomyocyte hypertrophy in the border zone of the infarction was, however, increased in G-CSF/SCF-treated hearts. Increased binding of G-CSF to its receptor on cardiomyocytes activates the Akt (34, 35) as well as the Jak/STAT

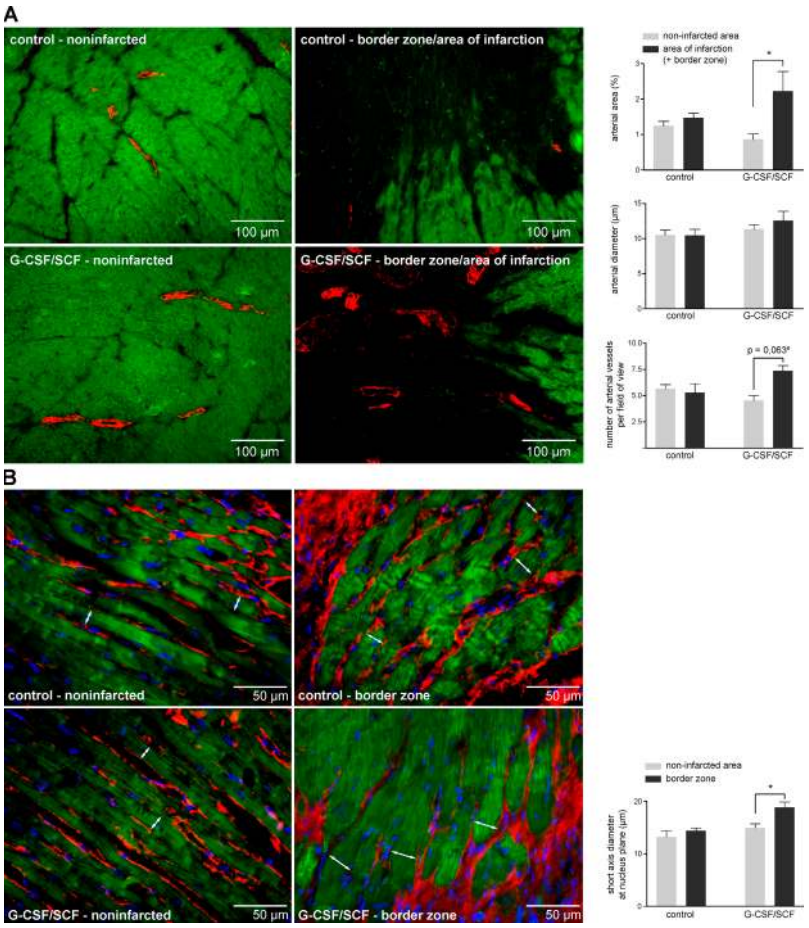

Figure 5. Influence of G-CSF/SCF on arterialization and cardiomyocyte diameter. (A) Increased arterialization of the area of infarction, including the border zone, in G-CSF/SCF-treated hearts. Left: In situ identification of arterial vessels, visualized by α-smooth muscle actin staining (red fluorescence) in the non-infarcted (left panels) and infarcted areas plus the border zone (right panels) of untreated (top panels) and G-CSF/SCF-treated hearts (bottom panels). Right: Quantitative analysis of arterialization. *, statistical significance of difference ($P < 0.05$); #, a p-value determined by performing a nonparametric test (Wilcoxon signed rank test) because a normality test failed. Performing the corresponding parametric test would lead to $P < 0.05$. (B) G-CSF/SCF increases cardiomyocyte diameter in the border zone of the infarction. Left: In situ detection of cardiomyocyte diameter in the non-infarcted areas (left panels) and in the border zone of infarction (right panels) of untreated (top panels) and G-CSF/SCF-treated hearts (bottom panels). Red fluorescence, cardiomyocyte boundaries; DAPI staining, nuclei; green autofluorescence, cardiomyocytes. Right: Quantitative analysis. There was no difference in normal myocardium between controls and G-CSF/SCF-treated hearts in normal myocardium, but cardiomyocyte diameter was increased in G-CSF/SCF-treated hearts in the border zone of the infarction.

pathway (14, 36), which are both known to impart hypertrophic signaling in cardiomyocytes. For the Akt pathway, it has also been demonstrated that its transgene-mediated, constitutive activation in mouse cardiomyocytes improves their contractile function in vitro as well as in vivo (37).

The increased vascularization in the border zone of the infarction (Fig. 5 A) might have also contributed to the improved cardiac output by enabling increased supply of oxygen and nutrients. Angiogenesis might be at least in part induced by direct effects of G-CSF, indicated by distinct immunolocalization of G-CSFR in vessel wall cells 1 d after induction of myocardial infarction. This finding is in accordance with Harada et al. (14), who detected G-CSFR expression in endothelial cells, and with Chen et al. (38), who demonstrated that G-CSF induces proliferation of vascular smooth muscle cells. Activation of the Akt as well as the Jak/STAT pathway by the binding of G-CSF to its receptor also might have been responsible for the enhanced induction of arteriogenesis in the G-CSF/SCF-treated hearts as suggested by work of Iwanaga et al. (39) and Harada et al. (14).

Lack of proarrhythmic effects of G-CSF/SCF

Despite the homing of a large number of BM-derived cells into the border zone of myocardial infarction (up to 30% of all nucleated cells), a dedicated protocol to provoke afterdepolarizations and ventricular arrhythmias did not provoke afterdepolarizations or spontaneous ventricular tachycardias in G-CSF/SCF-treated hearts. The lack of differentiation into myocytes of the majority of BM-derived cells, observed by us and others (17–19, 40), and consideration of the electrotonic attenuation of abnormal electrical behavior of a single cell when it is integrated into the myocardial syncytium, can explain that we did not find afterdepolarizations in the intact heart.

Reduced inducibility of ventricular arrhythmias

G-CSF/SCF-treated hearts had less inducible ventricular arrhythmias during programmed ventricular stimulation than controls (Fig. 4 B). Slow conduction due to decreased intercellular coupling in the border zone of a healed myocardial infarction is the pivotal factor for reentrant ventricular tachycardias in this setting (26, 41, 42). Reentry due to slow zigzag conduction in the border zone of an infarction is mainly caused by a dramatic decrease in expression of gap junctional proteins, specifically in connexin43 (26, 43). Indeed, a reduction of connexin43 expression by ~90% is sufficient to enhance inducibility of ventricular tachycardias in transgenic mice (44). A comparable (90%) reduction of connexin43 expression was found in cardiomyocytes in the border zone of the infarction in the absence of G-CSF/SCF treatment (Fig. 4 C). G-CSF/SCF partially reversed the down-regulation of connexin43 expression (Fig. 4 C) by increasing connexin43 levels in the border zone of the infarction to ~25% of normal expression. This level of connexin expression is sufficient to maintain almost normal conduction velocities (44) and can explain why G-CSF/SCF-treated hearts were protected against induction of ventricular tachyarrhythmias in this study.

This study examined the midterm electrophysiological effects of G-CSF/SCF into the infarcted myocardium. Arrhythmic events, including sudden arrhythmic death, may occur late after myocardial infarction, and current revascularization therapies during acute myocardial infarction usually limit infarct size in the clinical setting. The G-CSF/SCF treatment protocol was chosen here in agreement with the pioneering work by Orlic et al. (10) to allow for comparison of our data with those published by this group. Further studies are needed to establish a protocol for BM mobilization that is clinically applicable, i.e., where treatment begins during the acute phase of a myocardial infarction.

In summary, our data suggest that G-CSF/SCF has beneficial functional hemodynamic, electrophysiological, and microstructural effects in the absence of formation of new myocardium from BM-derived cells.

MATERIALS AND METHODS

Animals. 114 mice, which were 58 CD1 outbred mice (Charles River Deutschland GmbH; body weight 23–30 g at the day of myocardial infarction) and 56 female C57BL/6 inbred mice (Charles River Deutschland GmbH; body weight 20–26 g at the day of BMT), were studied. C57BL/6 mice served as hosts for BM transplantation from EGFP-expressing transgenic donor mice (also C57BL/6 background; reference 45). These mice were used to analyze myocardial homing of BM-derived cells. All experiments were performed in accordance with the German Law on the Care and Use of Laboratory Animals and were approved by the local Institutional Review Board.

Transplantation of EGFP-expressing BM-derived cells and splenectomy. To investigate the effect of G-CSF/SCF on mobilization and myocardial homing of BM-derived cells, 34 recipient mice underwent total body irradiation at a dose of 11 Gy (0.98 Gy/min), and intravenous infusion of BM (2×10^7 mononuclear cells) was harvested from EGFP-expressing mice the next day. The procedural details have been described previously (46). Blood cell chimerism determined 8 wk after BMT by FACS analysis showed >95% donor cells ($EGFP^+$) in all transplanted mice. Myocardial homing of BM-derived cells was studied 10 wk after BMT.

With the exception of eight C57BL/6 animals only used for the analysis of BM mobilization in nonsplenectomized mice, all experimental animals were splenectomized according to a published protocol (10) at least 2 wk before BMT or G-CSF/SCF treatment in non-BMT animals.

G-CSF/SCF treatment and induction of myocardial infarction. Recombinant mouse SCF (50 μg/kg/day; R&D Systems) and recombinant human G-CSF (200 μg/kg/day; Chugai Pharma Marketing Ltd.) were injected subcutaneously for 6 d. Control mice received daily injections of 0.9% saline. On the third day of G-CSF/SCF treatment, myocardial infarction was induced by ligation of the proximal LAD. To investigate basal accumulation of EGFP-expressing BM-derived cells in the myocardium, in 10 BMT animals (5 G-CSF/SCF-treated and 5 controls) no myocardial infarction was induced. For additional information see the supplemental Materials and methods, available at http://www.jem.org/cgi/content/full/jem.20051151/DC1.

Five G-CSF/SCF mice and four controls with EGFP-expressing BM (see above) were killed 24 h after induction of myocardial infarction (fourth day of G-CSF/SCF treatment) to determine the expression of G-CSFR. The hearts of all other animals were analyzed 5 wk after ligation of the LAD (animals with myocardial infarction) or the third day of G-CSF/SCF treatment (animals without myocardial infarction).

White blood cell analysis. After 4 d of G-CSF/SCF treatment, 200 μl blood was obtained from the tail vein of 31 animals (15 controls and 16 treated with G-CSF/SCF). Automatic full blood count measurements using the KK-21 hematology analyzer (Sysmex GmbH) were performed. After Pappenheim staining of blood smears, the proportion of lymphocytes, neutrophils, and monocytes in at least 100 white blood cell counts was calculated.

Echocardiography and surface ECG recordings. Sedated mice (ketamine/xylazine) underwent Doppler echocardiographic studies 5 wk after infarction immediately before the electrophysiological study according to published procedures (47). For additional details, see the supplemental Materials and methods.

Electrophysiological study in isolated hearts. The heart was excised under general anesthesia, and the aorta was cannulated and retrogradely perfused using 37°C Krebs-Henseleit buffer (in mmol/liters; NaCl 118, NaHCO3 24.88, KH2PO 41.18, glucose 5.55, Na-pyruvate 2, MgSO4 0.83, CaCl2 1.8, KCl 4.7) equilibrated with a 95% oxygen/5% carbon dioxide gas mixture. The heart was mounted on a vertical Langendorff apparatus (Hugo Sachs Electronic-Harvard Apparatus GmbH) and constantly perfused at 100 ± 5 mmHg perfusion pressure, corresponding to coronary flow rates of 4 ± 1 ml/min. An octapolar mouse electrophysiologic catheter (CIBER MOUSE; NuMED) was placed in the right atrium and ventricle for atrial and ventricular pacing. A tissue bath ECG was recorded from Ag-AgCl electrodes immersed in superfused sponges flanking the isolated heart. Three murine monophasic action potentials (MAPs) were continuously and simultaneously recorded from the right and left ventricular epicardium (23–25). One MAP was positioned within the border zone of the infarct to record afterdepolarizations. All recordings were obtained simultaneously throughout the experimental protocols. ECG signals were amplified and filtered by an ECG amplifier at a bandwidth of 0.1 to 300 Hz (Hugo Sachs Electronic-Harvard Apparatus GmbH). MAP signals were amplified using dedicated MAP amplifiers (Boston Scientific Inc.). Additional details of the experimental setup have been described previously (23–25).

After placing all catheters in a stable position, atrial pacing was performed at different pacing cycle lengths to measure steady-state action potential durations. To provoke ventricular arrhythmias initiated by afterdepolarizations, the atrioventricular node was ablated and the spontaneous ventricular rhythm was observed for 10 min (23, 24). Thereafter, to test the propensity to reentry, programmed ventricular stimulation was performed using up to two premature stimuli (S2 and S3) at different pacing cycle lengths (80–140 ms; reference 48). All signals were digitized at 1 or 2 KHz and stored on digital media for offline analysis.

Histology and immunofluorescence. After completion of the electrophysiologi25cal procedure, hearts were either fixed in Bouin's solution and stained using Goldner's Trichrom staining, or fixed in 3.7% formaldehyde, followed by dehydration in 10% sucrose solution, O.C.T. embedding, and cryoconservation for fluorescent detection of EGFP-expressing cells or immunofluorescent detection of various antigens according to an established protocol (49). The following primary antibodies were used: rat anti–mouse CD45 as a marker for blood cells (AB3088; Abcam Limited), monoclonal anti–troponin T as a marker of differentiated cardiomyocytes (cardiac isoform AB-1, clone 13-11; Lab Vision), rabbit anti–rat connexin43 polyclonal antibodies for the detection of gap junctions (71-0700; Zytomed GmbH), monoclonal rat anti-reticular fibroblast antibodies (clone ER-TR7; Novus Biologicals Inc.), rabbit smooth muscle anti-actin antibody for the detection of arteries and arterioles (RB-9010; Lab Vision Corporation), rabbit c-kit (SCF receptor) antibody (sc-168; Santa Cruz Biotechnology, Inc.), and rabbit anti–G-CSFR antibody (sc-694; Santa Cruz Biotechnology, Inc.). For additional information see the supplemental Materials and methods.

Sections were examined using a confocal fluorescence microscope (Axioplan 2 and LSM 510 Meta; Carl Zeiss MicroImaging, Inc.). Images were digitized and transferred to a personal computer. For quantification of different cell populations, the number of $EGFP^+$ cells and of $EGFP^+$ cells coexpressing the immunohistological marker (anti-CD45 or anti–troponin T antibody) were counted in three randomly selected fields of view at the same magnification (400) in the infarcted area, the border zone, and in the noninfarcted area of the left ventricle. For quantitative analysis of connexin expression, the number of $connexin43^+$ spots and the proportion of the $connexin43^+$ area in relation to the nonfibrotic myocardial area of the respective field of view were determined on digitized images taken at high magnification (400) from at least two nonconsecutive slides per mouse heart (four control and five G-CSF/SCF-treated animals) using Adobe Photoshop CS (Adobe Systems GmbH) and ImageJ 1.32 imaging software (National Institute of Mental Health). A minimum of eight images from the border zone and the non-infarcted area was analyzed in each heart.

Quantitative analysis of the arterial vessel area (smooth muscle $anti\text{-}actin^+$ area of vessels and enclosed lumina) was analyzed as described for the measurement of the $connexin43^+$ area (see above). In addition, the number of arterial vessels per field of view as well as the diameter of each vessel per field of view were determined.

Histological sections immunostained for fibroblasts/connective tissue were also used for short axis diameter measurement of cardiomyocytes at the nuclear level (100 cells per region and animal) using published methods (50) adapted for immunofluorescence; i.e., DAPI staining was used for the detection of nuclei and cardiomyocytes were identified based on their autofluorescence.

RNA isolation and real-time RT-PCR. Infarcted hearts of male CD1 mice at different time points after surgery (30 min, $n = 2$; 1 h, $n = 3$; 4 h, $n = 3$; 24 h, $n = 2$; 1wk, $n = 2$; 6 wk, $n = 3$) were explanted and the area of infarction, including its border zone, was separated from the non-infarcted myocardial tissue. Ventricular tissues of seven explanted hearts of untreated male CD1 mice served as controls.

Isolation of RNA from mouse heart tissue was performed using the RNeasy Fibrous Tissue Mini kit (QIAGEN) according to the manufacturer's protocol. Reverse transcription was performed using the ImProm-IITM Reverse Transcription System (Promega) according to the manufacturer's protocol. cDNA samples reverse transcribed from RNAs were analyzed by quantitative RT-PCR using primers (see the supplemental Materials and methods) purchased from MWG-BIOTECH AG. Quantitative RT-PCR was performed using SYBR Green Reaction Mix (Eurogentec) on an ABI PRISM 7900HT Detection System (Applied Biosystems). Each sample was run in duplicate. The expression of each gene within the different tissue samples was quantified relative to cyclophilin A expression according to the Sequence Detector User Bulletin 2 (Applied Biosystems).

Statistics. All procedures and analyses (functional and histological) were performed by a blinded experimenter with respect to treatment group (G-CSF/SCF vs. control). Depending on the existence of equal variances and normal distribution of data, treatment groups were compared using an unpaired *t* test and one-way ANOVA, respectively, or the corresponding nonparametric test procedures (Mann-Whitney U test and Kruskal-Wallis test). A chi-square test and log rank test were used to compare nominal parameters (e.g., inducibility of arrhythmias or mortality).

Online supplemental material. QuickTime videos (Videos S1–S4) presenting 3D-animated sequences of confocal scans of myocardial sections immunolabeled for connexin43/connective tissue (same scale as in Fig. 4 C) and supplemental Materials and methods are available at http://www.jem.org/cgi/content/full/jem.20051151/DC1.

We thank Karin Wacker, Reinhard Kiefer, Sezen Maleki, Angela Nigmann, Sergiu Scobioala, Daniela Volkery, Jürgen Sindermann, and Wolf-Rüdiger Schäbitz for expert assistance. We also thank Chugai Pharma Marketing Ltd. (Frankfurt am Main, Germany) for providing the rhG-CSF.

This study was supported in part by the Interdisciplinary Center for Clinical Research Münster (project ZPG4a to P. Kirchhof, L. Fabritz, and J. Stypmann), the

Stem Cell Network NRW, Ministry9 for Science and Research of Northrhine Westphalia, Düsseldorf, Germany (to M. Kuhlmann and S. Nikol), and by a grant of the Gesellschaft zur Förderung der Westfälischen Wilhelms-Universität, Münster, Germany (to S. Nikol).

The authors have no conflicting financial interests.

Submitted: 7 June 2005
Accepted: 28 November 2005

REFERENCES

1. Kannel, W.B. 2000. The Framingham Study: ITS 50-year legacy and future promise. *J. Atheroscler. Thromb.* 6:60–66.
2. Cowie, M.R., D.A. Wood, A.J. Coats, S.G. Thompson, P.A. Poole-Wilson, V. Suresh, and G.C. Sutton. 1999. Incidence and aetiology of heart failure; a population-based study. *Eur. Heart J.* 20:421–428.
3. Wood, D.A. 2002. Preventing clinical heart failure: the rationale and scientific evidence. *Heart.* 88:ii15–ii22.
4. Chamberlain, D.A. 1987. Overview of completed sudden death trials: European experience. *Cardiology.* 74:10–23.
5. Myerburg, R.J., K.M. Kessler, and A. Castellanos. 1992. Sudden cardiac death. Structure, function, and time-dependence of risk. *Circulation.* 85: I2–10.
6. Demirovic, J., and R.J. Myerburg. 1994. Epidemiology of sudden coronary death: an overview. *Prog. Cardiovasc. Dis.* 37:39–48.
7. Wollert, K.C., G.P. Meyer, J. Lotz, S. Ringes-Lichtenberg, P. Lippolt, C. Breidenbach, S. Fichtner, T. Korte, B. Hornig, D. Messinger, et al. 2004. Intracoronary autologous bone-marrow cell transfer after myocardial infarction: the BOOST randomised controlled clinical trial. *Lancet.* 364:141–148.
8. Assmus, B., V. Schachinger, C. Teupe, M. Britten, R. Lehmann, N. Dobert, F. Grunwald, A. Aicher, C. Urbich, H. Martin, et al. 2002. Transplantation of Progenitor Cells and Regeneration Enhancement in Acute Myocardial Infarction (TOPCARE-AMI). *Circulation.* 106: 3009–3017.
9. Kang, H.J., H.S. Kim, S.Y. Zhang, K.W. Park, H.J. Cho, B.K. Koo, Y.J. Kim, D. Soo Lee, D.W. Sohn, K.S. Han, et al. 2004. Effects of intracoronary infusion of peripheral blood stem-cells mobilised with granulocyte-colony stimulating factor on left ventricular systolic function and restenosis after coronary stenting in myocardial infarction: the MAGIC cell randomised clinical trial. *Lancet.* 363:751–756.
10. Orlic, D., J. Kajstura, S. Chimenti, F. Limana, I. Jakoniuk, F. Quaini, B. Nadal-Ginard, D.M. Bodine, A. Leri, and P. Anversa. 2001. Mobilized bone marrow cells repair the infarcted heart, improving function and survival. *Proc. Natl. Acad. Sci. USA.* 98:10344–10349.
11. Ohtsuka, M., H. Takano, Y. Zou, H. Toko, H. Akazawa, Y. Qin, M. Suzuki, H. Hasegawa, H. Nakaya, and I. Komuro. 2004. Cytokine therapy prevents left ventricular remodeling and dysfunction after myocardial infarction through neovascularization. *FASEB J.* 18: 851–853.
12. Minatoguchi, S., G. Takemura, X.H. Chen, N. Wang, Y. Uno, M. Koda, M. Arai, Y. Misao, C. Lu, K. Suzuki, et al. 2004. Acceleration of the healing process and myocardial regeneration may be important as a mechanism of improvement of cardiac function and remodeling by postinfarction granulocyte colony-stimulating factor treatment. *Circulation.* 109:2572–2580.
13. Sugano, Y., T. Anzai, T. Yoshikawa, Y. Maekawa, T. Kohno, K. Mahara, K. Naito, and S. Ogawa. 2005. Granulocyte colony-stimulating factor attenuates early ventricular expansion after experimental myocardial infarction. *Cardiovasc. Res.* 65:446–456.
14. Harada, M., Y. Qin, H. Takano, T. Minamino, Y. Zou, H. Toko, M. Ohtsuka, K. Matsuura, M. Sano, J. Nishi, et al. 2005. G-CSF prevents cardiac remodeling after myocardial infarction by activating the Jak-Stat pathway in cardiomyocytes. *Nat. Med.* 11:305–311.
15. Orlic, D., J. Kajstura, S. Chimenti, I. Jakoniuk, S.M. Anderson, B. Li, J. Pickel, R. McKay, B. Nadal-Ginard, D.M. Bodine, et al. 2001. Bone marrow cells regenerate infarcted myocardium. *Nature.* 410:701–705.
16. Orlic, D., J. Kajstura, S. Chimenti, D.M. Bodine, A. Leri, and P. Anversa. 2001. Transplanted adult bone marrow cells repair myocardial infarcts in mice. *Ann. NY Acad. Sci.* 938:221–229.
17. Murry, C.E., M.H. Soonpaa, H. Reinecke, H. Nakajima, H.O. Nakajima, M. Rubart, K.B. Pasumarthi, J.I. Virag, S.H. Bartelmez, V. Poppa, et al. 2004. Haematopoietic stem cells do not transdifferentiate into cardiac myocytes in myocardial infarcts. *Nature.* 428:664–668.
18. Balsam, L.B., A.J. Wagers, J.L. Christensen, T. Kofidis, I.L. Weissman, and R.C. Robbins. 2004. Haematopoietic stem cells adopt mature haematopoietic fates in ischaemic myocardium. *Nature.* 428:668–673.
19. Nygren, J.M., S. Jovinge, M. Breitbach, P. Sawen, W. Roll, J. Hescheler, J. Taneera, B.K. Fleischmann, and S.E. Jacobsen. 2004. Bone marrow-derived hematopoietic cells generate cardiomyocytes at a low frequency through cell fusion, but not transdifferentiation. *Nat. Med.* 10:494–501.
20. Gnecchi, M., H. He, O.D. Liang, L.G. Melo, F. Morello, H. Mu, N. Noiseux, L. Zhang, R.E. Pratt, J.S. Ingwall, and V.J. Dzau. 2005. Paracrine action accounts for marked protection of ischemic heart by Akt-modified mesenchymal stem cells. *Nat. Med.* 11:367–368.
21. Menasché, P., A.A. Hagege, J.T. Vilquin, M. Desnos, E. Abergel, B. Pouzet, A. Bel, S. Sarateanu, M. Scorsin, K. Schwartz, et al. 2003. Autologous skeletal myoblast transplantation for severe postinfarction left ventricular dysfunction. *J. Am. Coll. Cardiol.* 41:1078–1083.
22. He, J.Q., Y. Ma, Y. Lee, J.A. Thomson, and T.J. Kamp. 2003. Human embryonic stem cells develop into multiple types of cardiac myocytes: action potential characterization. *Circ. Res.* 93:32–39.
23. Fabritz, L., P. Kirchhof, M.R. Franz, L. Eckardt, G. Monnig, P. Milberg, G. Breithardt, and W. Haverkamp. 2003. Prolonged action potential durations, increased dispersion of repolarization, and polymorphic ventricular tachycardia in a mouse model of proarrhythmia. *Basic Res. Cardiol.* 98:25–32.
24. Fabritz, L., P. Kirchhof, M.R. Franz, D. Nuyens, T. Rossenbacker, A. Ottenhof, W. Haverkamp, G. Breithardt, E. Carmeliet, and P. Carmeliet. 2003. Effect of pacing and mexiletine on dispersion of repolarisation and arrhythmias in DeltaKPQ SCN5A (long QT3) mice. *Cardiovasc. Res.* 57:1085–1093.
25. Kirchhof, P., L. Fabritz, A. Kilic, F. Begrow, G. Breithardt, and M. Kuhn. 2004. Ventricular arrhythmias, increased cardiac calmodulin kinase II expression, and altered repolarization kinetics in ANP receptor deficient mice. *J. Mol. Cell. Cardiol.* 36:691–700.
26. Peters, N.S., J. Coromilas, N.J. Severs, and A.L. Wit. 1997. Disturbed connexin43 gap junction distribution correlates with the location of reentrant circuits in the epicardial border zone of healing canine infarcts that cause ventricular tachycardia. *Circulation.* 95:988–996.
27. Kudo, M., Y. Wang, M.A. Wani, M. Xu, A. Ayub, and M. Ashraf. 2003. Implantation of bone marrow stem cells reduces the infarction and fibrosis in ischemic mouse heart. *J. Mol. Cell. Cardiol.* 35: 1113–1119.
28. Bel, A., E. Messas, O. Agbulut, P. Richard, J.L. Samuel, P. Bruneval, A.A. Hagege, and P. Menasche. 2003. Transplantation of autologous fresh bone marrow into infarcted myocardium: a word of caution. *Circulation.* 108:II247–II252.
29. Lord, B.I., L.B. Woolford, and G. Molineux. 2001. Kinetics of neutrophil production in normal and neutropenic animals during the response to filgrastim (r-metHu G-CSF) or filgrastim SD/01 (PEG-r-metHu G-CSF). *Clin. Cancer Res.* 7:2085–2090.
30. Adachi, Y., J. Imagawa, Y. Suzuki, K. Yogo, M. Fukazawa, O. Kuromaru, and Y. Saito. 2004. G-CSF treatment increases side population cell infiltration after myocardial infarction in mice. *J. Mol. Cell. Cardiol.* 36:707–710.
31. Schneider, A., C. Krueger, T. Steigleder, D. Weber, C. Pitzer, R. Laage, J. Aronowski, M. Maurer, N. Gassler, W. Mier, et al. 2005. The hematopoietic factor G-CSF is a neuronal ligand that counteracts programmed cell death and drives neurogenesis. *J. Clin. Invest.* 115: 2083–2098.
32. Leone, A.M., S. Rutella, G. Bonanno, A.M. Contemi, D.G. de Ritis, M.B. Giannico, A.G. Rebuzzi, G. Leone, and F. Crea. 2005. Endogenous G-CSF and CD34(+) cell mobilization after acute myocardial infarction. *Int. J. Cardiol.* In press.
33. Deten, A., H.C. Volz, S. Clamors, S. Leiblein, W. Briest, G. Marx, and H.G. Zimmer. 2005. Hematopoietic stem cells do not repair the infarcted mouse heart. *Cardiovasc. Res.* 65:52–63.

34. Dong, F., and A.C. Larner. 2000. Activation of Akt kinase by granulocyte colony-stimulating factor (G-CSF): evidence for the role of a tyrosine kinase activity distinct from the Janus kinases. *Blood*. 95:1656–1662.
35. Matsui, T., L. Li, J.C. Wu, S.A. Cook, T. Nagoshi, M.H. Picard, R. Liao, and A. Rosenzweig. 2002. Phenotypic spectrum caused by transgenic overexpression of activated Akt in the heart. *J. Biol. Chem*. 277:22896–22901.
36. Kunisada, K., E. Tone, Y. Fujio, H. Matsui, K. Yamauchi-Takihara, and T. Kishimoto. 1998. Activation of gp130 transduces hypertrophic signals via STAT3 in cardiac myocytes. *Circulation*. 98:346–352.
37. Kim, Y.K., S.J. Kim, A. Yatani, Y. Huang, G. Castelli, D.E. Vatner, J. Liu, Q. Zhang, G. Diaz, R. Zieba, et al. 2003. Mechanism of enhanced cardiac function in mice with hypertrophy induced by overexpressed Akt. *J. Biol. Chem*. 278:47622–47628.
38. Chen, X., S.E. Kelemen, and M.V. Autieri. 2004. AIF-1 expression modulates proliferation of human vascular smooth muscle cells by autocrine expression of G-CSF. *Arterioscler. Thromb. Vasc. Biol*. 24:1217–1222.
39. Iwanaga, K., H. Takano, M. Ohtsuka, H. Hasegawa, Y. Zou, Y. Qin, K. Odaka, K. Hiroshima, H. Tadokoro, and I. Komuro. 2004. Effects of G-CSF on cardiac remodeling after acute myocardial infarction in swine. *Biochem. Biophys. Res. Commun*. 325:1353–1359.
40. Lapidos, K.A., Y.E. Chen, J.U. Earley, A. Heydemann, J.M. Huber, M. Chien, A. Ma, and E.M. McNally. 2004. Transplanted hematopoietic stem cells demonstrate impaired sarcoglycan expression after engraftment into cardiac and skeletal muscle. *J. Clin. Invest*. 114:1577–1585.
41. Luke, R.A., and J.E. Saffitz. 1991. Remodeling of ventricular conduction pathways in healed canine infarct border zones. *J. Clin. Invest*. 87: 1594–1602.
42. de Bakker, J.M., F.J. van Capelle, M.J. Janse, S. Tasseron, J.T. Vermeulen, N. de Jonge, and J.R. Lahpor. 1993. Slow conduction in the infarcted human heart. 'Zigzag' course of activation. *Circulation*. 88:915–926.
43. Abraham, M.R., C.A. Henrikson, L. Tung, M.G. Chang, M. Aon, T. Xue, R.A. Li, B. O'Rourke, and E. Marban. 2005. Antiarrhythmic engineering of skeletal myoblasts for cardiac transplantation. *Circ. Res*. 97: 159–167.
44. van Rijen, H.V., D. Eckardt, J. Degen, M. Theis, T. Ott, K. Willecke, H.J. Jongsma, T. Opthof, and J.M. de Bakker. 2004. Slow conduction and enhanced anisotropy increase the propensity for ventricular tachyarrhythmias in adult mice with induced deletion of connexin43. *Circulation*. 109:1048–1055.
45. Okabe, M., M. Ikawa, K. Kominami, T. Nakanishi, and Y. Nishimune. 1997. 'Green mice' as a source of ubiquitous green cells. *FEBS Lett*. 407:313–319.
46. Stelljes, M., R. Strothotte, H.G. Pauels, C. Poremba, M. Milse, C. Specht, J. Albring, G. Bisping, C. Scheffold, T. Kammertoens, et al. 2004. Graft-versus-host disease after allogeneic hematopoietic stem cell transplantation induces a CD8+ T cell-mediated graft-versus-tumor effect that is independent of the recognition of alloantigenic tumor targets. *Blood*. 104:1210–1216.
47. Gergs, U., P. Boknik, I. Buchwalow, L. Fabritz, M. Matus, I. Justus, G. Hanske, W. Schmitz, and J. Neumann. 2004. Overexpression of the catalytic subunit of protein phosphatase 2A impairs cardiac function. *J. Biol. Chem*. 279:40827–40834.
48. Fabritz, L., P. Kirchhof, M.R. Franz, D. Nuyens, T. Rossenbacker, A. Ottenhof, W. Haverkamp, G. Breithardt, E. Carmeliet, and P. Carmeliet. 2003. Effect of pacing and mexiletine on dispersion of repolarisation and arrhythmias in hearts of DeltaKPQ SCN5A (long QT3) mice. *Cardiovasc. Res*. 57:1085–1093.
49. Mueller, M., K. Wacker, W.F. Hickey, E.B. Ringelstein, and R. Kiefer. 2000. Co-localization of multiple antigens and specific DNA. A novel method using methyl methacrylate-embedded semithin serial sections and catalyzed reporter deposition. *Am. J. Pathol*. 157:1829–1838.
50. Sabrane, K., M.N. Kruse, L. Fabritz, B. Zetsche, D. Mitko, B.V. Skryabin, M. Zwiener, H.A. Baba, M. Yanagisawa, and M. Kuhn. 2005. Vascular endothelium is critically involved in the hypotensive and hypovolemic actions of atrial natriuretic peptide. *J. Clin. Invest*. 115: 1666–1674.